

AN LTCC-BASED CAPACITIVE PRESSURE SENSOR WITH A DIGITAL OUTPUT

Marina Santo Zarnik¹, Matej Možek², Srečko Maček³, Darko Belavič¹

¹HIPOT-RR d.o.o., Otočec, Slovenia

²Faculty of Electrical Engineering, University of Ljubljana, Ljubljana, Slovenia

³Jožef Stefan Institute, Ljubljana, Slovenia

Key words: Pressure sensor, 3-D LTCC structure, capacitive sensing, capacitive-to-digital conversion, low power consumption.

Abstract: A capacitive pressure sensor, fabricated using low-temperature cofired ceramic (LTCC) materials and technology was considered for an application in a wireless sensor system. LTCC technology is inherently efficient for 3D structuring and exhibits good dimensional definition and stability, appropriate material flexibility (higher than the commonly used alumina), good chemical resistance, and low moisture absorption, which makes it appropriate for a wide range of sensor applications, even in some extreme conditions and harsh environments. However, very often in such applications, remote control and operation in a low power-consumption mode are required. In order to meet such demands, electronics for signal processing and power managing, based on a capacitance-to-digital conversion, were realised by using an Analog Devices AD7746. A sensor characterization system with the corresponding software for an evaluation of the sensor's nonlinearity and temperature sensitivity is presented. The typical characteristics of the capacitive sensing elements were as follows: a sensitivity of 1.7 fF/mbar, a temperature dependence of 9 fF/°C and a temperature dependence of the sensitivity of less than 2 aF/mbar/°C. The digital temperature compensation was performed with a two-dimensional rational polynomial approximation, resulting in a less than 0.4% FS temperature error in the compensation range 10 °C to 75 °C.

Kapacitivni senzor tlaka z digitalnim izhodom izdelan v LTCC tehnologiji

Ključne besede: senzor tlaka, 3-D LTCC struktura, kapacitivni senzor, kapacitivno digitalna pretvorba, nizka poraba.

Izveček: V prispevku so prikazani rezultati študije kapacitivnega keramičnega senzorja tlaka za uporabo v brezžičnem senzorskem sistemu. Senzor je izdelan z uporabo keramike z nizko temperaturo žganja (LTCC – low temperature cofired ceramic) in z ustreznimi novimi tehnološkimi postopki. LTCC materiali in tehnologija so primerni za oblikovanje tri-dimenzionalnih keramičnih struktur. Poleg tega imajo LTCC materiali približno trikrat nižji Youngov modul elastičnosti v primerjavi z najpogosteje uporabljano korundno keramiko, kar omogoča doseganje večje tlačne občutljivosti senzorja. Zahvaljujoč še nekaterim drugim lastnostim, kot so kemična stabilnost in nizka absorpcija vlage, je LTCC keramika zelo primerna za uporabo v različnih medijih in celo v nekaterih ekstremnih pogojih. Pogosto je pri tovrstni uporabi potrebno zagotoviti tudi prenos in obdelavo merilnih rezultatov v oddaljeni enoti ob energijsko varčnem delovanju. V ta namen smo tudi izbrali kapacitivni senzorski princip, ki je že v osnovi energijsko varčen. Pretvorba in procesiranje senzorskega signala je izvedena z uporabo kapacitivno-digitalnega pretvornika AD7746. Predstavljen je merilni sistem z ustrežno programsko podporo za evaluacijo temperaturne kompenzacije senzorske karakteristike. Tipične karakteristike izmerjenih prototipov so naslednje: tlačna občutljivost je 1.7 fF/mbar, temperaturna odvisnost ničelne kapacitivnosti je 9 fF/°C in temperaturna odvisnost občutljivosti je manjša od 2 aF/mbar/°C. Z digitalno kompenzacijo temperaturne odvisnosti odziva smo dosegli napako manjšo od 0,4% FS na kalibracijskem temperaturnem področju 10 °C do 75 °C.

1. Introduction

Thick-film ceramic pressure sensors have been used for many years in a variety of special applications /1, 2/. One advantage of such ceramic sensors is that they can be employed in severe environments: such as high temperatures, magnetic fields, harsh atmospheres and in some aggressive liquids. Realised with the use of Low Temperature Cofired Ceramic (LTCC) materials and technology and offering advantageous features for 3D structuring /3/ (structures with cavities and channels, and buried electronic components, such as conductors, resistors or other functional layers) they have the potential to be an alternative to micro-machined sensors in silicon /6-9/. The most common application is a diaphragm-type ceramic pressure sensor. Depending on the sensing principle, the pressure-induced deformation of the thin ceramic diaphragm is converted into an electrical signal, which is proportional to the changes of the characteristics of the thick-film sensing structure on it (thick-film piezoresistors, thick-film piezoelectric structures or a capacitive sensing structure). The

appropriate electronics for the sensors' signal processing can be realised directly on the ceramic structure, i.e., the 3D ceramic structure can be used as a package substrate at the same time.

In order to ensure low power consumption, the capacitive sensing principle is one of the most appropriate methods /4-5/. In addition, the ceramic capacitive sensors have further advantages: a very high sensitivity and, accordingly, a potentially high resolution, robustness, good stability, and drift-free measurement capability. However, they traditionally require more complex interfacing circuits, which represented a major disadvantage in the past. Generally, the capacitive sensing utilises the deformation-induced capacitance change to convert the information of the applied pressure into the electrical signal, such as changes of the oscillation frequency, time, charge, and voltage. The translation from voltage or current to a digital word requires an additional analogue-to-digital converter (ADC). The expected variance in capacitance is generally of the order of several pF or less. In many cases the signal capacitance is

much smaller than the parasitic capacitances present in the measuring circuit, which represents a difficult interfacing task. However, a modification of the conventional sigma delta ADC architecture has been identified as a suitable basis for a monolithic Capacitance to Digital Converter (CDC) /12/. The circuit is parasitic insensitive, and can be configured to work with both a floating and a grounded configuration /16/.

Precision capacitive-sensor interface products are based on a well-established sigma-delta ($\Sigma\Delta$) conversion technology. Converters utilizing the $\Sigma\Delta$ principle offer excellent linearity and very high resolution, and are ideal for most sensor-interfacing applications. In a conventional voltage input $\Sigma\Delta$ converter, the unknown charge is derived from charging a fixed capacitor to an unknown input voltage, while in the CDC realization, the voltage is fixed and the capacitor is variable. Such an arrangement maintains the high precision and accuracy that is typical for $\Sigma\Delta$ ADCs /13/. Modern implementations enable the measurement of capacitances in the atto Farad (aF) range /15, 16/, with an effective noise resolution of 21 bits and a corresponding resolution down to 4aF. They offer measurements of common-mode capacitance up to 17pF on the 4pF range with a 4fF measurement accuracy. These implementations offer complete sensor solutions; however, their application is limited to an indication of temperature and by the humidity dependence problem /17, 18/ of capacitive sensors, while not offering an effective implementation for the compensation of these unwanted quantities.

This work reports on the results of a case study of a thick-film capacitive pressure-sensor module made with LTCC technology. The electronics for the signal processing and power managing, based on a capacitance-to-digital conversion, were realised with the use of an Analog Devices AD7746, which was placed directly on the ceramic structure, close to the sensing capacitor electrodes. The sensor is connected via an interface module to the I²C - USB converter, which is used to interface the sensor to the host computer (PC). The prototype sensors were characterised in the pressure range 0-1 bar. The stability and the temperature dependence of the sensors' characteristics were discussed and an effective method for temperature compensation is presented. The sensor nonlinearity and temperature sensitivity were analyzed. In order to achieve the compensation and linearization, an effective method of temperature compensation based on a two-dimensional rational polynomial description of the sensor characteristic was employed.

2 Ceramic capacitive pressure sensors

2.1 Theory of capacitive sensing

The construction of the LTCC-based capacitive pressure sensor consists of a circular, edge-clamped deformable

diaphragm that is bonded to a rigid ring and the base substrate. One electrode deposited on the rigid substrate and one electrode deposited on the deformable diaphragm form a parallel-plate air-gap capacitor. The operation of the capacitive pressure sensor is based on changing the air gap between the electrodes as a result of the applied pressure (Figure 1).

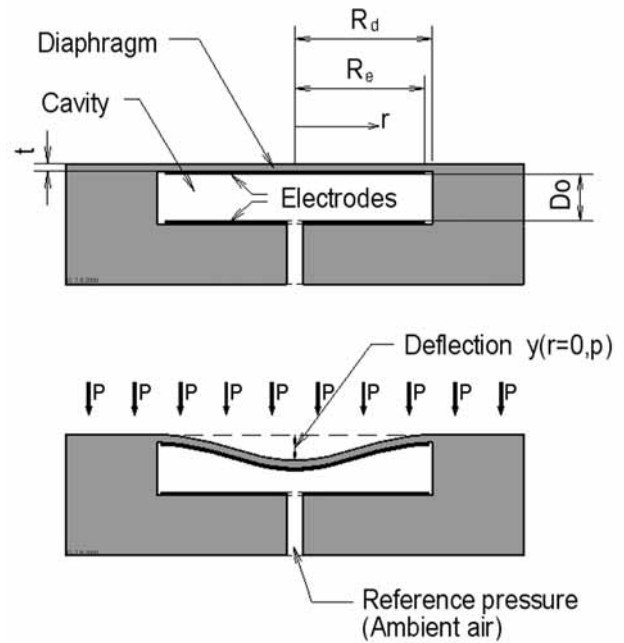


Fig. 1: The construction of the capacitive pressure sensor (above). The deflection of the diaphragm under the measuring pressure applied to the exterior surface of the diaphragm (below).

The capacitance between the electrodes on the deflected diaphragm and the rigid substrate can be expressed with equation (1)

$$C(p) = \epsilon_0 \cdot \epsilon_r \cdot \int_0^{R_e} \frac{2 \cdot \pi \cdot r \cdot dr}{D_0 - y(r, p)} \quad (1)$$

where ϵ_0 and ϵ_r are the dielectric permittivity of free space and the relative dielectric permittivity of the dielectric, R_e is the radius of the electrode, r is the distance from the centre of the electrode/diaphragm, D_0 is the distance between the electrodes at zero pressure, p is the measuring pressure and $y(r, p)$ is the deflection of the diaphragm when the pressure is applied. For a clamped circular diaphragm $y(r, p)$ can be calculated from (2)

$$y(r, p) = \frac{3p(1-\nu^2)(R_d^2 - r^2)^2}{16Et^3} \quad (2)$$

where t and R_d are the thickness and the radius of the diaphragm, E is the Young's modulus and ν is the Poisson's ratio of the diaphragm. Substituting equation (2) into (1) allows preliminary calculations of the sensitivity in the sensor's design phase. Notice that depending on how the pressure is applied, i.e., on the exterior surface of the diaphragm or in the interior of the cavity (or equivalently, if the pressure or an under-pressure is applied), $y(r, p)$ with a

positive or negative sign should be considered. However, the sensor's sensitivity to the applied pressure depends on the area of the electrodes and the initial distance between them. Accordingly, the realization of a very small distance between the electrodes is essential if we are to achieve a high resolution.

2.2 LTCC-based capacitive sensing structure

In a typical capacitive pressure-sensor construction the thick-film ceramic pressure sensor consists of a ceramic capsule, i.e., a cylindrical cavity (air gap), closed with a thin flexible ceramic diaphragm parallel to a rigid reference substrate. The thick-film electrodes of the sensing capacitor were made on the diaphragm and the substrate plane inside the cavity in co-processing with the LTCC structure. The cross-section of the LTCC-based capacitive pressure sensor considered in this case study is schematically presented in Figure 2. The important dimensions of the prototype sensors were as follows: a diaphragm diameter of 9 mm and a thickness of 200 μm , an electrode diameter of 8.5 mm, and air gap between the electrodes of 50-70 μm . Such a sensor provides a total capacitance change of approximately 1.5 pF for an applied pressure in the range of 0-1 bar. A detail of the parallel-plate air-gap capacitor (cross-section of the LTCC-based sensor structure) is shown in Figure 3. Figure 4 shows the prototype of the LTCC-based capacitive pressure-sensor module with AD7746/45. In order to minimise the stray capacitances that adversely influence the sensitivity to the pressure loads the CDC was placed on the same ceramic substrate, as close as possible to the capacitor electrodes. In this realisation the top surface of the diaphragm is covered with a 3- μm -thick Au film with the same dimensions as the electrode inside the ceramic capsule.

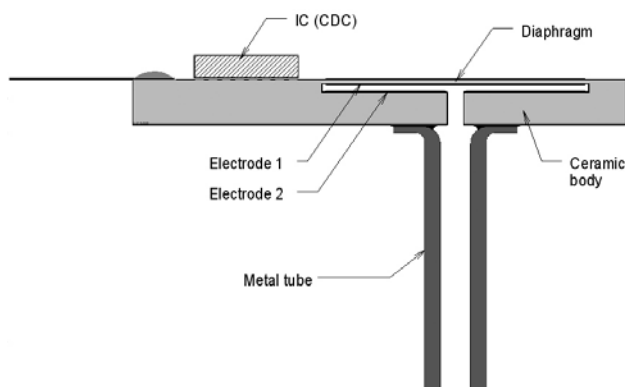


Fig. 2: Schematic representation of the cross-section of the sensor structure (not to scale)

3. Capacitive sensor characterization systems

The generalized layout of the capacitive-sensor measurement system is depicted in Figure 5. The sensor is con-

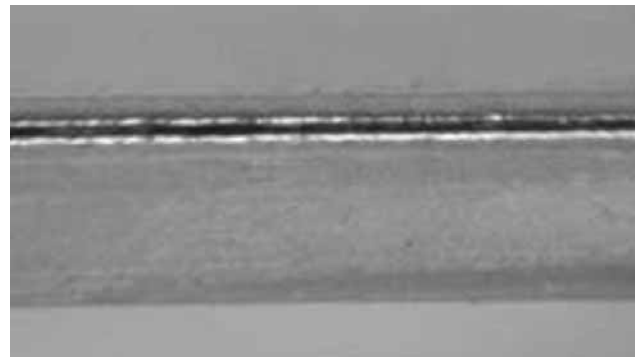


Fig. 3: A detail of the cross-section of the LTCC structure with the air gap between the cofired thick-film electrodes on the diaphragm and the rigid base.

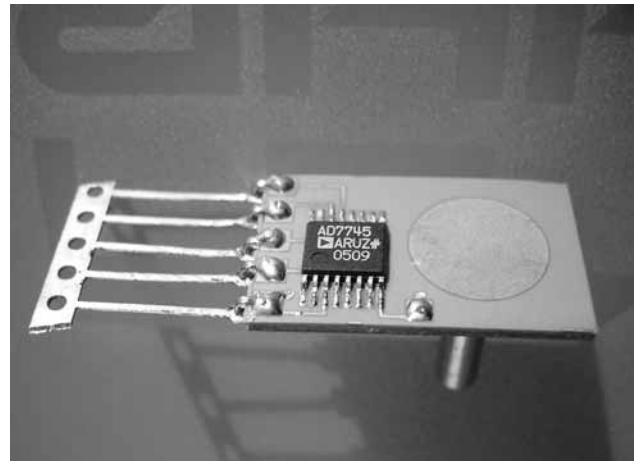


Fig. 4: Prototype of the capacitive ceramic pressure sensor with the AD7745.

nected via the interface module to the I²C - USB converter, which is used to interface the sensor to the host PC. A dedicated electronic interface module was designed. This module enables data transmission and the control of the CDC AD7746. The module itself is based on a CY8C24794 Programmable System on Chip (PSoC) circuit.

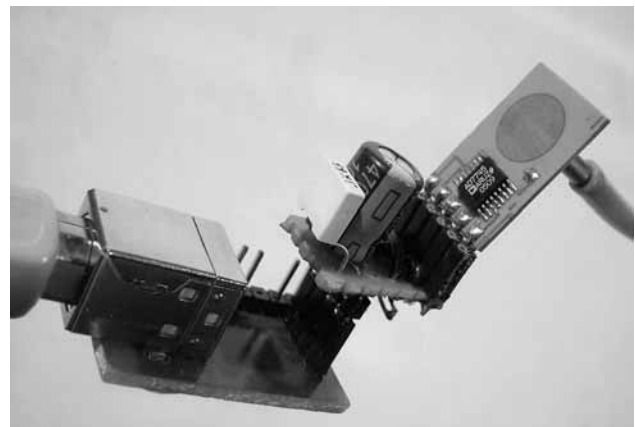


Fig. 5: Capacitive sensor evaluation module

The hardware is used to directly map the CDC to the controlling PC. The corresponding PC software performs the functions of CDC status and data reading. In fact, the controlling software implements all the functions of the AD7746: from the capacitance channel setup to the temperature sensor channel setup, as well as the channel excitation, the common mode capacitance setting, the offset and the gain of the capacitive measurement channel.

The measurement-range optimization was performed in order to obtain the maximum span of the CDC measurement range. The measured device, the LTCC capacitive sensor /18/, exhibits a negative slope for the sensor characteristic. Therefore, the measurement-range optimization must be performed at the maximum pressure readout with a minimum pressure applied and vice versa. This also imposes the order of the compensation algorithms, i.e., the offset compensation is performed before the gain compensation. The sensor offset response is compensated by setting the AD7746 registers CAPDACA and CAPOFFSET. The register value CAPDACA value affects the coarse setting of the offset response and the CAPOFFSET affects the fine setting of the sensor response. The procedure of offset setting is composed of the coarse and fine offset settings. Because of the negative sensor characteristic slope, the fine offset value is initially set at maximum and the coarse value is altered from its initial zero value in such manner that the sensor response is maintained at its maximum value. The setting of the CAPDACA register is performed by a successive approximation approach, starting at the MSB of the CAPDACA register. The subsequent bits are tested against the raw sensor output. If the sensor output exceeds the maximum sensor readout (FFFF₁₆) when the corresponding bit is set to 1, then the bit is set to zero and the algorithm advances towards the lower bits.

After the coarse register was set, the CAPOFFSET register is processed in a similar manner. The result of this algorithm is a maximum sensor response value at the applied offset pressure.

After a successful optimization of the offset value, the gain parameter is set in a similar manner. The minimum sensor response is set with an alteration of the CAPGAIN register, which actually changes the clock rate of the front-end of the CDC. The procedure starts with the minimum setting of the CAPGAIN register. The bits of the CAPGAIN register are tested according to the described successive approximation algorithm, just that the bit-testing criterion is now the minimum CDC readout. The result of this algorithm is a minimum sensor response at the maximum applied pressure.

From the capacitive channel output data, where the 0x000000 code represents the zero scale (0 pF), and the 0xFFFFFFFF code represents the full scale (+4.096 pF), the capacitance can be calculated using the following expressions:

$$C_{sens} = C_0 + C_{offset} + C_s \quad (3)$$

$$C_0 = \frac{Code}{128} \cdot 17 pF \quad (4)$$

$$C_{offset} = \frac{Code}{65536} \cdot 1 pF \quad (5)$$

$$C_s = (Code - 0xFFFFFFFF) \cdot C_{ref} \quad (6)$$

where the *Code* is the corresponding CDC readout and *C_{ref}* is 4.096 pF.

For the temperature sensor on a chip, the temperature can be calculated from the code (readout of the temperature channel) using the following equation /16/:

$$Temperature (^\circ C) = (Code / 2048) - 4096. \quad (7)$$

3.1. Characterisation of the ceramic capacitive-sensing structure

Initially, the measurements of the prototype sensor were performed for a determination of the optimal settings of the AD7746 and the tested LTCC capacitive sensing structure. The typical sensor characteristic, obtained in an up and down scan of the pressure range 0-700 mbar, at room temperature (25°C ± 0.5 °C) is presented in Figure 6. In order to assess the repeatability the up and down scans were repeated several times. It is evident from Figure 7 that the repeatability was very good and that the tested sensor exhibits practically no hysteresis. For the pressure loads up to 300 mbar the characteristic is almost linear (R² = 0.9998), and only for a wider pressure range, over 1 bar, does the deviation from an ideal straight line indicate the necessity for sensor characteristic linearization.

From the CDC readouts the capacitance was calculated using formula (3). As a result, the variation of the capacitance over the pressure range was assessed, which showed a typical sensitivity of 1.8 fF/mbar.

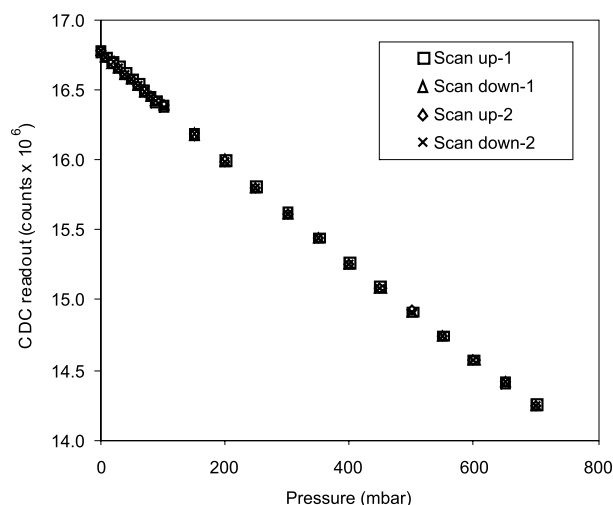


Fig. 6: Initial measurements of the randomly selected test sensor characteristics

In the following, the resolution and the temperature dependence of the sensor's characteristics were measured.

The sensor and the interface electronic circuit were placed in the temperature chamber and the measurement of the raw response was repeated at different temperatures for the temperature range 10-75 °C and for a relative humidity of the air of 30 %. A minimum temperature of 10 °C was selected for the initial measurements in order to avoid potential problems with the humidity control and freezing at the lower temperatures, and to limit affecting the sensors characteristics due to the temperature and humidity dependence of the permittivity of air. These measurements also revealed the susceptibility of the initial electronic circuit design to electromagnetic interference and pointed out the necessity for further improvement of the design in future. During the measurements at the stabilized temperatures in the temperature chamber, switching of the chamber compressor affected the sensor readout and impaired the signal-to-noise ratio.

Figure 7 shows the readouts from the CDC for continuous measurements of the unloaded sensor (C_0), and the ambient temperature, obtained from the on-chip temperature sensor by using relation (7), for the compressor switched ON and OFF. According to Figure 7, the peak-to-peak noise of the sensors signal measured for the compressor switched on was almost two times higher than in the case when the compressor was switched off. Being aware of this effect we continued the characterisation of the capacitive sensing element for its temperature compensation for the stabilised readouts.

The stabilized raw CDC readouts obtained at the different temperatures for different pressure loads are presented in Figure 8. Figure 9 shows the temperature dependence of the sensor with no pressure applied.

The typical characteristics obtained from measurements of several sensing elements (expressed in terms of the capacitance changes) were as follows: the average sensitivity was 1.7 fF/mbar, the temperature dependence of the sensor with no pressure applied, C_0 , was 9 fF/°C and the temperature dependence of the sensitivity was less than 2 aF/mbar/°C. The sensors exhibited practically no hysteresis. However, the deviation from an ideal straight line for the wider pressure range and the temperature dependence of the sensor's characteristic indicated the necessity for characteristic linearization.

3.2 Temperature compensation

As the CDC produces a digital capacitance readout, we focused our work on digital implementations of the temperature compensations. In the case of the investigated pressure sensor the temperature compensation requires an accurate mathematical description of the sensor's characteristic pressure and temperature axis. The most adaptable and versatile digital description of the sensor characteristic is achieved with a Taylor expansion, recommended by the IEEE1541.2 standard [19]. Its major drawback is the use of floating-point calculation coefficients and an

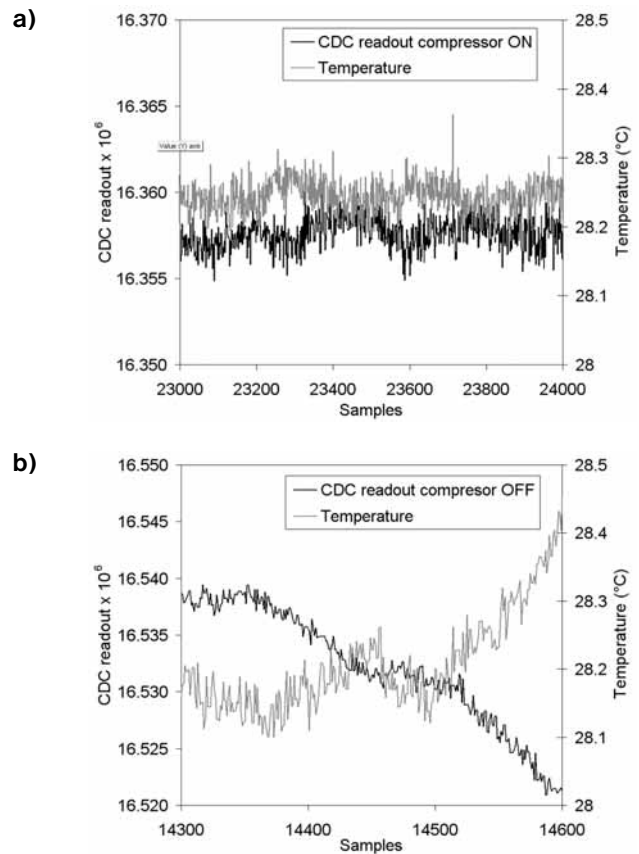


Fig. 7 a: CDC response of C_0 versus number of samples measured with the compressor switched ON, b: CDC response of C_0 versus number of samples measured with the compressor switched OFF

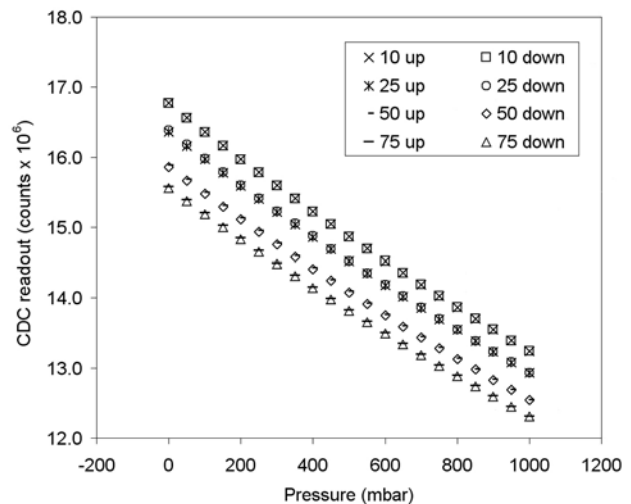


Fig. 8: CDC readouts versus pressure characteristics (for the pressure sweep up and down) at the different temperatures

orthogonal mesh of calibration points. The degree of approximating the polynomial defines the size of the calibration point mesh.

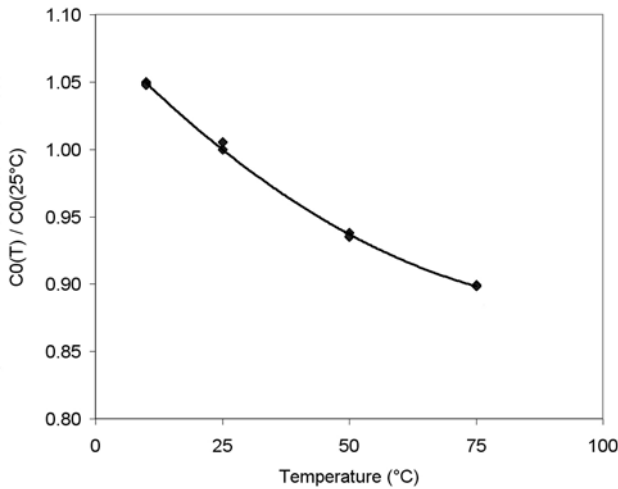


Fig. 9: The temperature characteristic of the sensor output with no pressure applied (C_0) measured in the temperature range -25°C to 75°C .

In order to accommodate the above-mentioned drawbacks, the temperature variations of a typical sensor characteristic can be described by means of a rational polynomial description (8), where A_0 through A_6 are the calibration coefficients of the pressure sensor, which effectively covers the sensor nonlinearity in the pressure and temperature direction to the second order.

$$p = \frac{A_0 + \Delta P + A_1 \cdot \Delta P^2 + A_2 \cdot \Delta T + A_3 \cdot \Delta T^2}{A_4 + A_5 \cdot \Delta T + A_6 \cdot \Delta T^2} \quad (8)$$

Note that in a given formulation of the characteristic description, the actual temperature and capacitance readouts have only an indirect significance on the final measured quantity p , since the calculation of (8) does not depend on the actual value of the capacitance or temperature.

Pressure and temperature measurements are represented by an offset-corrected raw pressure and temperature value. The Δp represents an offset-corrected raw readout from the capacitive sensor, ΔT represents the offset-corrected raw readout from the temperature sensor residing on the sensor signal conditioner. In order to minimize the calibration error, the raw pressure readout p_{oc} and the raw temperature readout T_{oc} are offset according to equation (9) by the corresponding values $p_{ocOFFSET}$ and $T_{ocOFFSET}$ respectively.

$$\begin{aligned} \Delta p &= p_{oc} - p_{ocOFFSET} \\ \Delta T &= T_{oc} - T_{ocOFFSET} \end{aligned} \quad (9)$$

The solution for the unknown coefficients $A_0 \dots A_6$ can be found by solving a system of linear equations, obtained from the calibration data. The calibration points for a given sensor are ordered into a seven-point calibration scenario. The calibration scenario represents a sequence of calibration points, comprised of boundary values that define the pressure and temperature calibration interval. The scenario is constructed by setting three temperature points,

and pressure points at the endpoints of the corresponding calibration interval. In the case of the presented sensor, the following calibration points were obtained with the pressure-sensor characterization system.

3.2.1 Temperature-compensation evaluation

Software for the acquisition, analysis and calibration of the capacitive sensors was designed. Table 1 summarizes the evaluation of the experimental data depicted in Figure 6. Seven calibration points were used for the evaluation of the calibration coefficients.

Table 1: Input calibration data.

CP#	P_{CAL} (mbar)	T ($^\circ\text{C}$)	p_{OC}	T_{OC}
1	0	10	32746	16424
2	1000	10	25858	16424
3	0	50	30995	16584
4	500	50	27512	16584
5	1000	50	24492	16584
6	0	75	30405	16684
7	1000	75	24037	16684

Additional test points were obtained during the acquisition stage of the calibration process. Test points were obtained at 10°C , 25°C , 50°C and 75°C in the interval from 0 mbar to 1000 mbar in 50 mbar steps, resulting in a set of 175 test points, which were used in the evaluation process for an assessment of the temperature error.

The calibration dataset was taken from the calibration points in Table 1 and the coefficients were determined. Equation (9) was evaluated at the test points in Table 2. The calibration error, ϵ , was calculated using the expression

$$\epsilon = \left| \frac{P_{CAL} - P_{EVAL}}{FS} \right| \cdot 100\% \quad (10)$$

where P_{CAL} represents the calibration pressure point, P_{EVAL} represents the evaluation pressure and FS represents the output pressure span. The evaluation of the system of linear equations based on equation (10) yields the calibration coefficients summarized in Table 2.

Table 2: Calculated calibration coefficients.

A_0	A_1	A_2	A_3	A_4	A_5	A_6
-6547	-1703	5148	-4246	-29413	-1307	1990

Equation (9) was evaluated at 175 test-points gathered during the acquisition process using the calibration coefficients in Table 2. The pressure and temperature offset values $p_{ocOFFSET}$ and $T_{ocOFFSET}$ were selected at 30000 and 16500 respectively. The results are summarized in Figure 10, which shows the calibration error ϵ calculated using equation (10). Figure 3 also shows the upper and lower admissible calibration temperature error band for a typical sensor application.

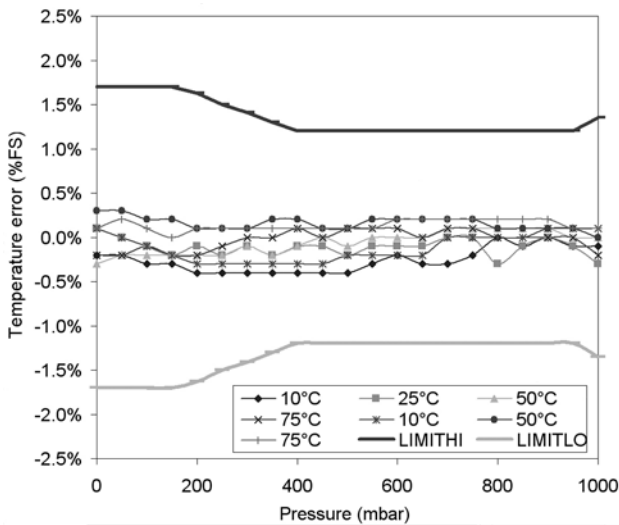


Fig. 10: Evaluation error at the test-point data.

An implementation of a digital temperature compensation method, developed for piezoresistive pressure sensors, to the field of capacitive sensors was presented in order to achieve an effective compensation and linearization based on a two-dimensional rational polynomial description. The evaluation results of the sensor response were compared against a reference pressure source and the most effective digital temperature compensation was proposed. The proposed digital compensation yields a maximum 0.4% FS error on the compensation range 10 °C to 75 °C and enables 16-bit integer arithmetic, thus making the proposed approach appropriate for use in modern sensor signal conditioner integrated circuits.

3.4 Power consumption

The power consumption was measured at different CDC settings. The supply current was obtained from measurements of the voltage drop in a 100-ohms serial resistor by using a LeCroy 9310C oscilloscope. The results obtained for the idle system and for two different sampling rates, i.e., 90 samples per second (SPS) and 9 SPS, are presented in Figure 11.

It was shown that the power consumption of the idle system of typically 2 mW at the supply voltage of 5V increased for a higher sample rate and did not exceed 5 mW in any case. A further reduction of the power consumption, generally attributed to the very lower clock frequency of the CDC, can be achieved only by turning off the CDC during inactive operation intervals.

4. Conclusions

A capacitive pressure sensor aimed at applications in a wireless sensor system was made using LTCC materials and technology. The tested prototype sensors proved to meet the functional demands imposed by the targeted application on a laboratory scale.

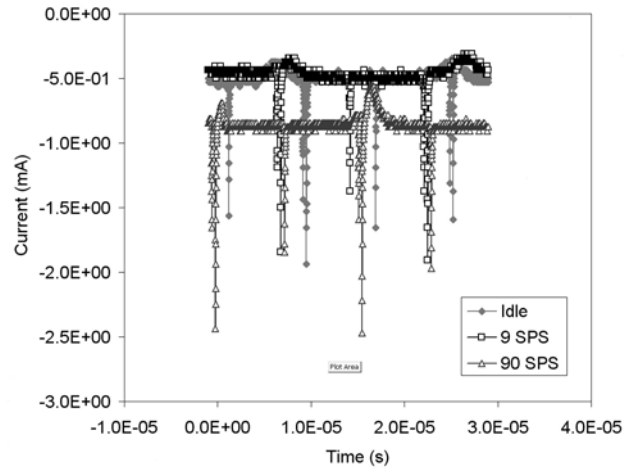


Fig. 11: The current measured for an idle CDC and for two different sampling rates

The typical characteristics of the capacitive sensing elements were as follows: a sensitivity of 1.7 fF/mbar, a temperature dependence of 9 fF/°C and a temperature dependence of the sensitivity of less than 2 aF/mbar/°C. The electronics for the sensor’s signal processing, based on the capacitance-to-digital conversion, was realised by use of an Analog Devices AD7746. The sensor characterization system with the corresponding software for evaluation of the sensor’s nonlinearity and the temperature sensitivity was built and tested. Digital temperature compensation, performed with a two-dimensional rational polynomial approximation, resulted in a typical temperature error of less than 0.4% FS on the compensation range 10 °C to 75 °C. This enables 16-bit integer arithmetic, making the proposed approach appropriate for use in modern sensor signal conditioner integrated circuits. The power consumption, estimated at the supply voltage of 5V, did not exceed 5 mW.

With smart power management, a significant reduction of the power consumption level and better power efficiency could be achieved in a continuation of this work.

5. Acknowledgements

The financial support of the Slovenian Research Agency and the company HYB d.o.o. in the frame of the project L2-O186 is gratefully acknowledged. The authors wish to thank Mr. Mitja Jerlah (from the HYB Company) for producing the test sensors.

Literature

- /1./ M. Prudenziati, editor, Handbook of Sensors and Actuators, vol. 1: Thick film sensors, Elsevier, 1994.
- /2./ N.M. White, J.D. Turner, Thick film sensors: past, present and future. Meas. Sci. Technol. 8, 1-20 (1997)
- /3./ K. A. Peterson, K. D. Patel. C. K. Ho, S. B. Rohde, C. D. Nordquist, C. A. Walker, B. D. Wroblewski, M. Okandan, Novel microsystem applications with new techniques in low-temperature

- co-fired ceramics, *Int. J. Appl. Ceram. Technol.*, 2, (5), (2005), 345-363
- /4./ R. Puers, "Capacitive sensors: when and how to use them", *Sensors and Actuators A*, 37-38 (1993) 93-105
- /5./ W. Bracke, R. Puers, C. Van Hoof, *Ultra Low power Capacitive Sensor Interfaces* Springer 2007.
- /6./ C. B. Sippola, C. H. Ahn, "A thick film screen-printed ceramic capacitive pressure microsensor for high temperature applications", *Journal of Micromechanics and Microengineering*, Vol.16, pp. 1086-1091, 2006.
- /7./ M.G.H Meijerik, E. Nieuwkoop, E.P. Veninga, M.H.H. Meuwissen, M.W.W.J. Tjeldink, "Capacitive pressure sensor in post-processing on LTCC substrates", *Sensors and Actuators A*, 123-124, 2005, 234-239
- /8./ S. T. Moe, K. Schjølberg-Henriksen, D. T. Wang, E. Lund, J. Nysaether, L. Furuberg, M. Visser, T. Fallet, R.W. Bernstein, *Capacitive differential pressure sensor for harsh environments*, *Sensors and Actuators* (2000) 30-33.
- /9./ G. Blasquez, X. Chauffleur, P. Pons, C. Douziech, P. Favaro, Ph. Menini, *Intrinsic thermal behaviour of capacitive pressure sensors: mechanisms and minimisation*, *Sensors and Actuators* 85 (2000) 56-69.
- /10./ L. K. Baxter, *Capacitive Sensors*, copyright 6-26-00, <http://www.capsense.com/capsense-wp.pdf>
- /11./ Winncy Y. Du, Scott W. Yelich, *Resistive and Capacitive Based Sensing Technologies*, *Sensors & Transducers*, ISSN 1726-5479, 2008, IFSA, http://www.sensorsportal.com/HTML/DIGEST/P_SI_29.htm
- /12./ S. R. Norsworthy, R. Schreier, G. C. Temes, "*Delta-Sigma Data Converters*" IEEE Press, 1997, Wiley-IEEE Press, ISBN: 978-0780310452
- /13./ J. C. Candy, G. C. Temes, "Oversampling Delta-Sigma data converters", IEEE Press, Publisher: Wiley-IEEE Press, 2008, ISBN: 978-0879422851
- /14./ O'Dowd, J. Callanan, A. Banarie, G. Company-Bosch, E "Capacitive sensor interfacing using sigma-delta techniques" *Sensors*, 2005 IEEE, pp.-951-954, ISBN: 0-7803-9056-3, Digital Object Identifier: 10.1109/ICSENS.2005.1597858
- /15./ M. Bingesser, Teddy Loeliger, Werner Hinn, Johann Hauer, Stefan Mödl, Robert Dorn, Matthias Völker "Low-noise sigma-delta capacitance-to-digital converter for Sub-pF capacitive sensors with integrated dielectric loss measurement" *Proceedings of the conference on Design, automation and test in Europe*, Munich, Germany, 2008, pp. 868-872.
- /16./ Analog Devices AD7746 Evaluation Board - EVAL-AD7746EB, Revision 0, May 2005. Available on: http://www.analog.com/static/imported-files/eval_boards/252730993EVAL_AD7746EB_0.pdf
- /17./ S. Pratt "Environmental Compensation on the AD7142: The Effects of Temperature and Humidity on Capacitance Sensors" *Analog Devices Application Note AN-829*, 2005. http://www.analog.com/static/imported-files/application_notes/5773153083373535958633AN829_0.pdf
- /18./ D. Belavič, M. S. Zarnik, M. Hrovat, S. Maček, M. Kosec, "Temperature behaviour of capacitive pressure sensor fabricated with LTCC technology" *Inf. MIDEM*, 2009, vol. 38, no. 3, pp. 191-196.
- /19./ IEEE Std. 1451.2 D3.05-Aug1997 "IEEE standard for a smart transducer interface for sensors and actuators – Transducer to microprocessor communication protocols and transducer electronic data sheet (TEDS) formats" *Institute of Electrical and Electronics Engineers*, September 1997.

Marina Santo Zarnik¹, Matej Možek²,
Srečko Maček³, Darko Belavič¹

¹HIPOT-RR d.o.o., 8222 Otočec, Slovenia

²Faculty of Electrical Engineering, 1000 Ljubljana,
University of Ljubljana, Slovenia

³Jožef Stefan Institute, 1000 Ljubljana, Slovenia

Prispelo (Arrived): 10.11.2009

Sprejeto (Accepted): 09.03.2010